Geophysical Research Letters

Supporting Information for

Is there a Nascent Plate Boundary in the Northern Indian Ocean?

A. Coudurier-Curveur[1,2], Ç. Karakaş[1,3], S. Singh[1,2], P. Tapponnier[1,4], H. Carton[2], and N. Hananto[5]

1 Earth Observatory of Singapore, Nanyang Technological University, 50 Nanyang Avenue, 639798 Singapore.

2 Équipe de Géosciences Marines, Institut de Physique du Globe de Paris (CNRS, Paris Diderot, Sorbonne Paris Cité), 1 rue Jussieu, 75238 Paris Cedex 05, France.

3 Schlumberger Research Center, Risabergvegen 3, 4068 Stavanger, Norway.

4 Institute of Crustal Dynamics, China Earthquake Administration, Haidian, Beijing, 100085, China.

5 Research Center for Oceanography, Indonesian Institute of Sciences, Jl Pasir Putih 1 Ancol Timur, Jakarta Utara 14430, Indonesia.

Contents of this file

Introduction

We present here second-order information on the methods, dataset, and calculations presented in this study.

Supplementary figures

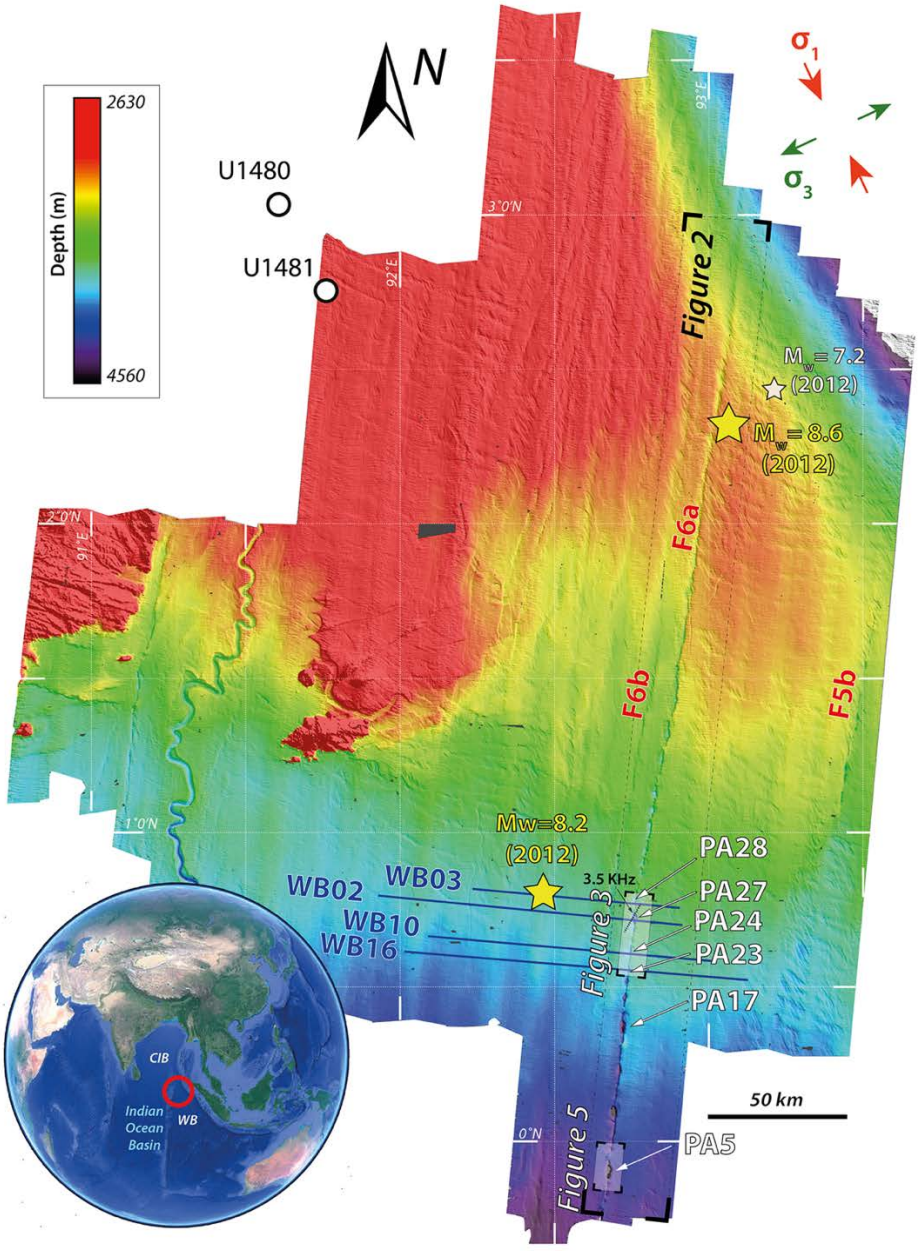

Figure S1. Geophysical dataset of the northern Wharton Basin. *EM122 multibeam bathymetry (colored DEM with depth) overlaid by M8+ 2012 earthquakes sequence (yellow stars), and Mw=7.2 (2012) earthquake (white star), seismic reflection profiles acquired during the MEGATERA scientific experiment (EW blue lines), 3.5 kHz profile across PA27 pull-apart (oblique black dash line) and location of the main pull-apart basins analyzed in this study. White and black*

circles indicate location of sedimentary cores recovered during IODP 362 expedition on board the R/V JOIDES Resolution (McNeill et al., 2017). Principal compressional (σ1) and extensional (σ3) stresses from Singh et al., 2017.

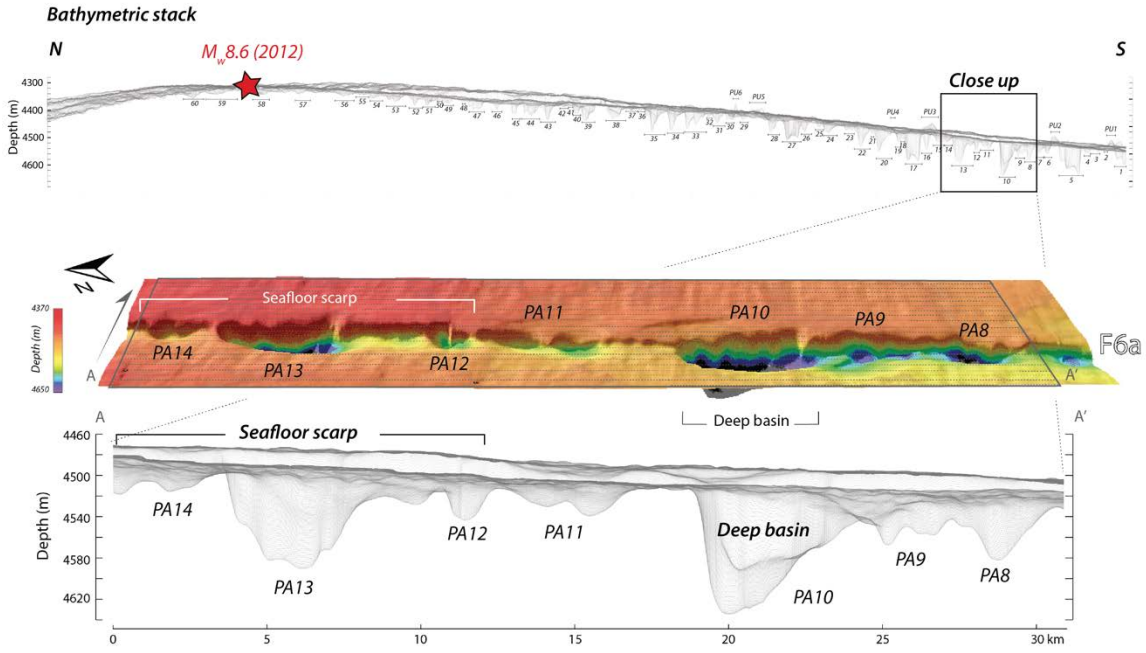

Figure S2. Bathymetric stack technique. *(Top) Bathymetric stack with pull-apart like basins labels. PA stands for pull-apart and PU for push-up. (Middle) Oblique view of bathymetric dataset between 0°2'N and 0°16'N with location of pull-apart basins 8 to 14 (from South to North). (Bottom) Bathymetric data and corresponding topographic stack highlighting pull-apart basins geometry. Each gray curve represents one bathymetric profile extracted from the bathymetric surface shown right above.*

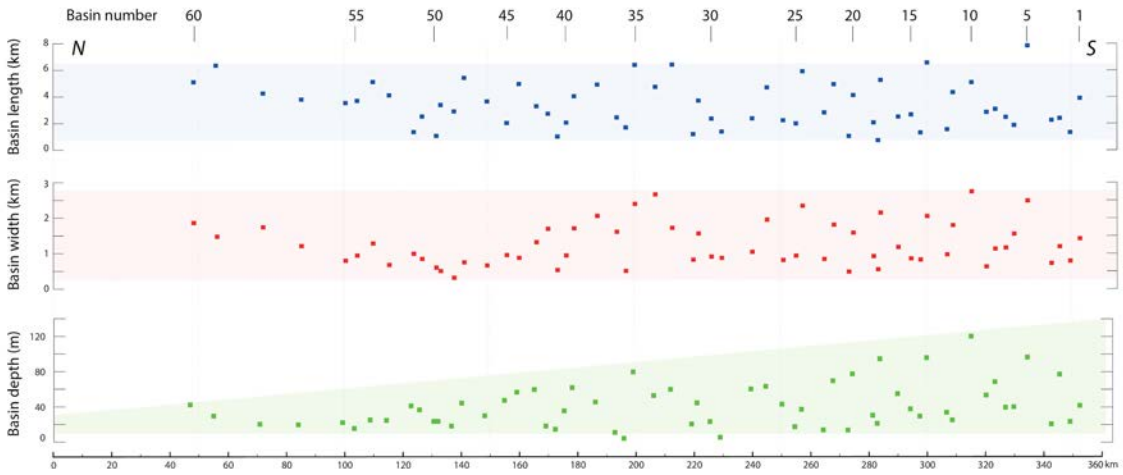

Figure S3. Along strike variations of geometric parameters for the 60 pull-apart like basins identified along the F6a fracture zone. *Length distribution (top) does not seem to follow any specific pattern along strike. Length is no smaller than 3500 m between PA53 and PA60. Small PA are mostly found in the South. Along-strike distribution of the pull-apart basin widths (middle) shows a wide dispersion between PA1 and PA43, where width ranges between ca.500 m and ca. 2600 m. Between PA 44 and PA56, width is smaller than 1300 m, and between PA57 and PA60, width is between 1200 m and 1900 m. Depth distribution (bottom) shows a decreasing trend from northward. Deepest basins located in the south; shorter basins with depths below 50 m (from PA48) in the north.*

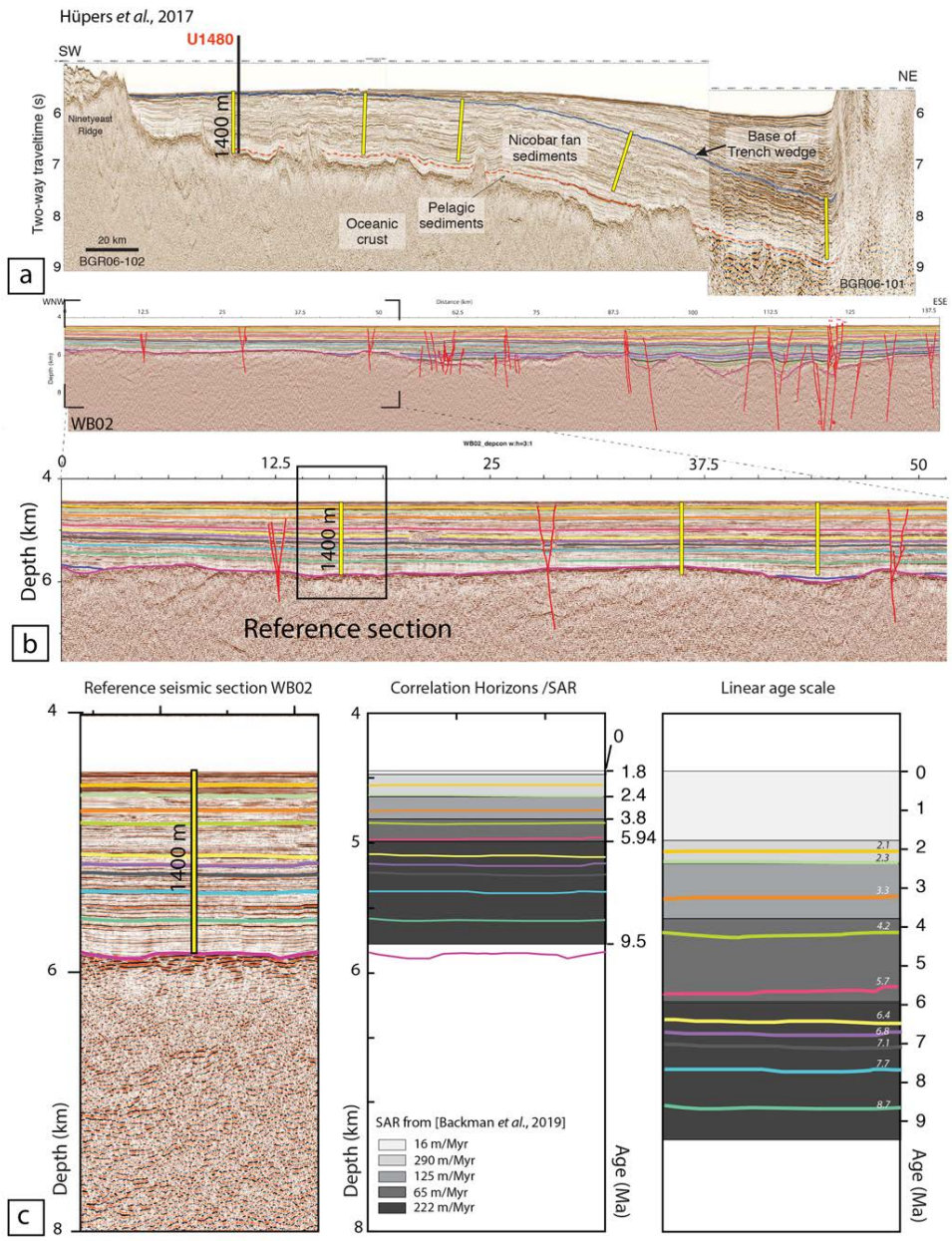

Figure S4. Site correlation and reflector age attribution using Sedimentation Accumulation Rates derived from U1480 biostratigraphic analyses. (*a). Seismic line acquired during IODP 362 scientific experiment showing U1480 core location (Hüpers et al., 2017). Yellow bars represent the 1400 m-long U1480 core and highlight sediment thickness variation along seismic line BGR06-101-102. (b). Full (top) and western section of (bottom) WB02 seismic line. Thickness of Nicobar Fan deposits away from deformed regions is similar to the U1480 core thickness. 1400 m thick reference section (black rectangle) is used to constrain age of reflectors within deformed regions, where thickness deposits varies (c). (Left) Reference section with 10 mapped reflectors. (Middle) Correlation of reflectors and deposit thickness derived from the 4 SAR periods determined by Backman et al. (2019). Age limits for these 4 periods are indicated on the right side. (Right) Reflectors and age correlation with a linear time scale.*

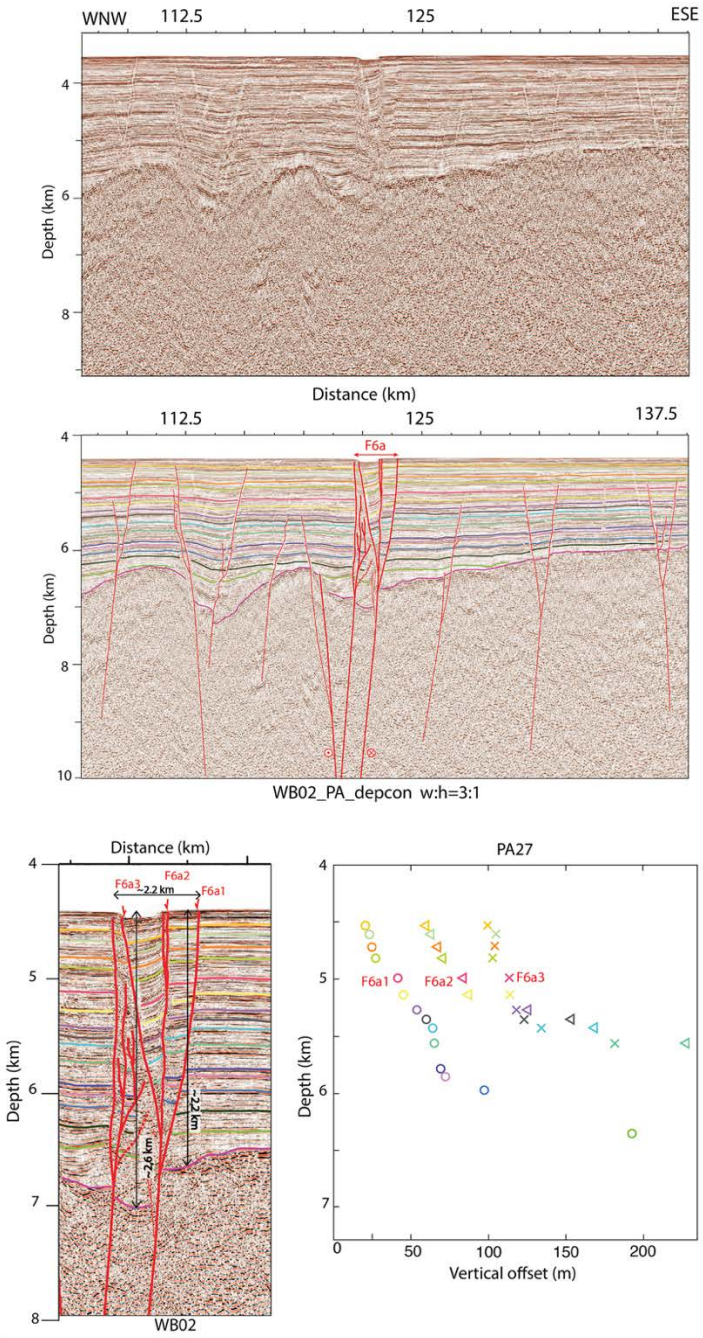

Figure S5. Seismic profile WB02 and associated cumulative vertical offset as a function of depth in the pull-apart basin 27. *(Top) Raw and interpreted profile WB02. (Bottom left) Key interpretation of seismic profile WB02 highlights reflectors, corresponding to the Nicobar fan deposits and to the basement, cut and offset by three splays of the F6a (1,2, and 3) fracture zone. Top of the oceanic basement displays pronounced high and low reliefs (i.e., ridges and depressions, respectively) and corresponds as the transition between the chaotic facies of the oceanic crust unit below and mostly continuous, sub-parallel reflections of the sedimentary cover above. (Bottom right) Vertical offset of the 15 mapped reflectors as a function of depth (km).*

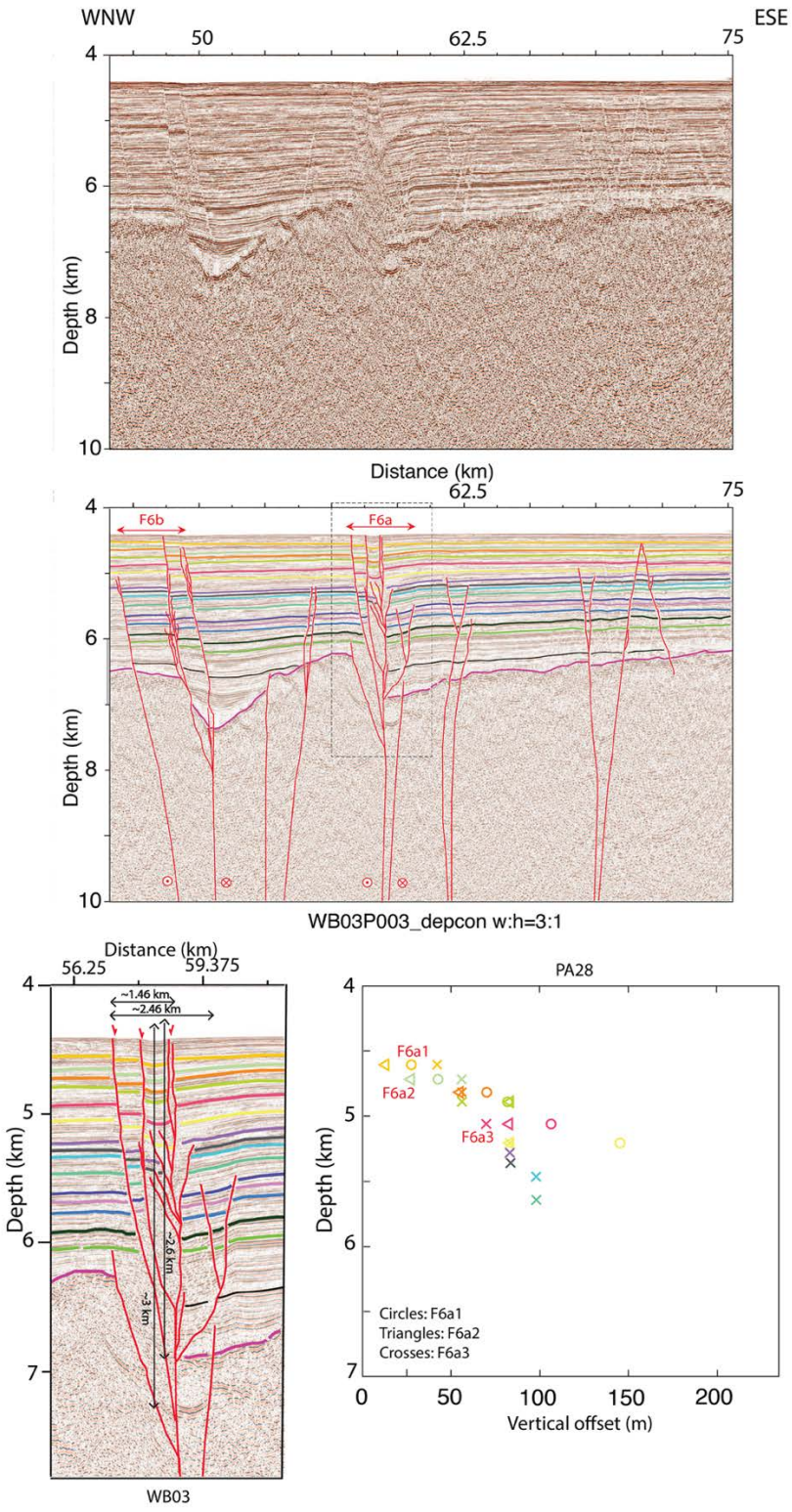

Figure S6. Seismic profile WB03 and associated cumulative vertical offset as a function of depth in the pull-apart basin 28. *PA 28 pull-apart structure comparable to PA27 with ≈ 3km thick sedimentary cover cut by three main splays of the F6a fracture zone.*

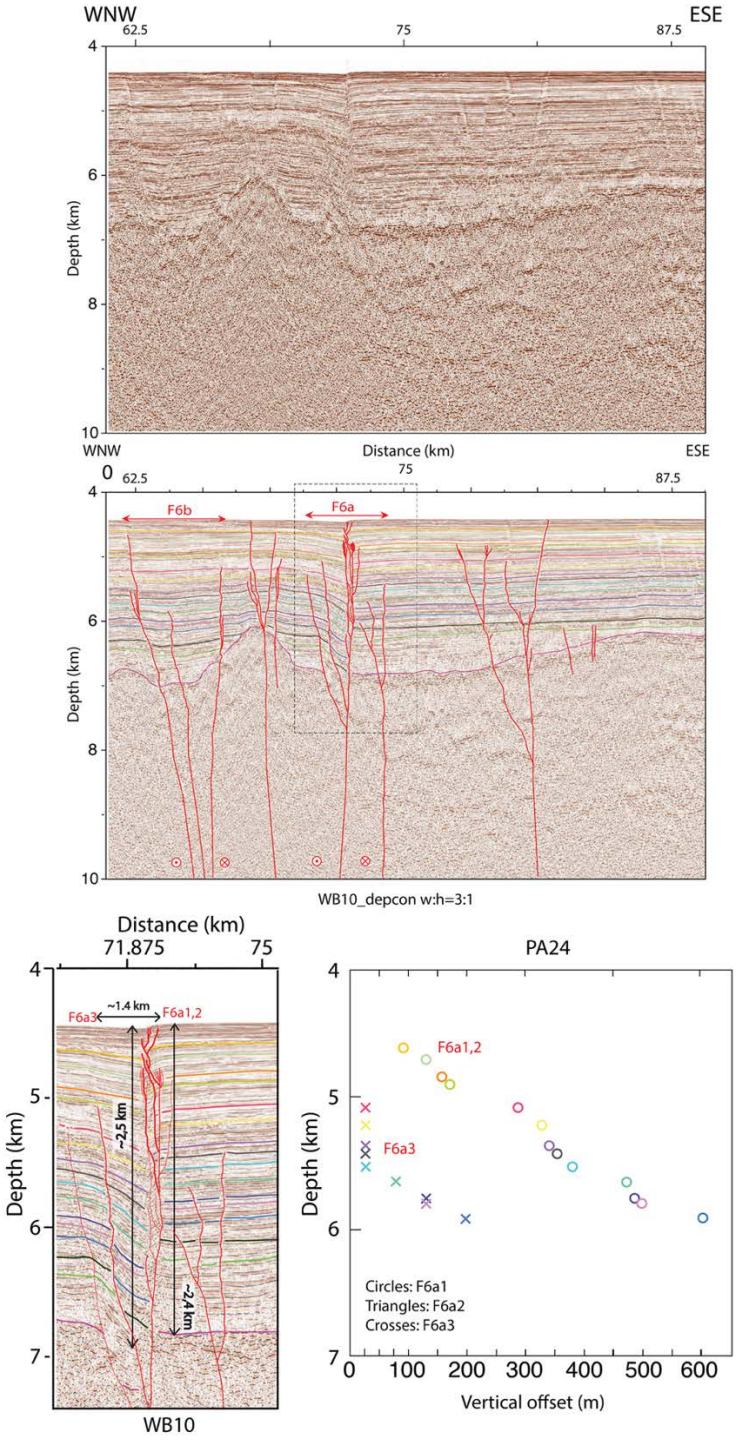

Figure S7. Seismic profile WB10 and associated cumulative vertical offset of reflectors as a function of depth in the pull-apart-like basin 24. *Two to three splays of the main F6a fault are visible on the WB10 profile and in the bathymetry.*

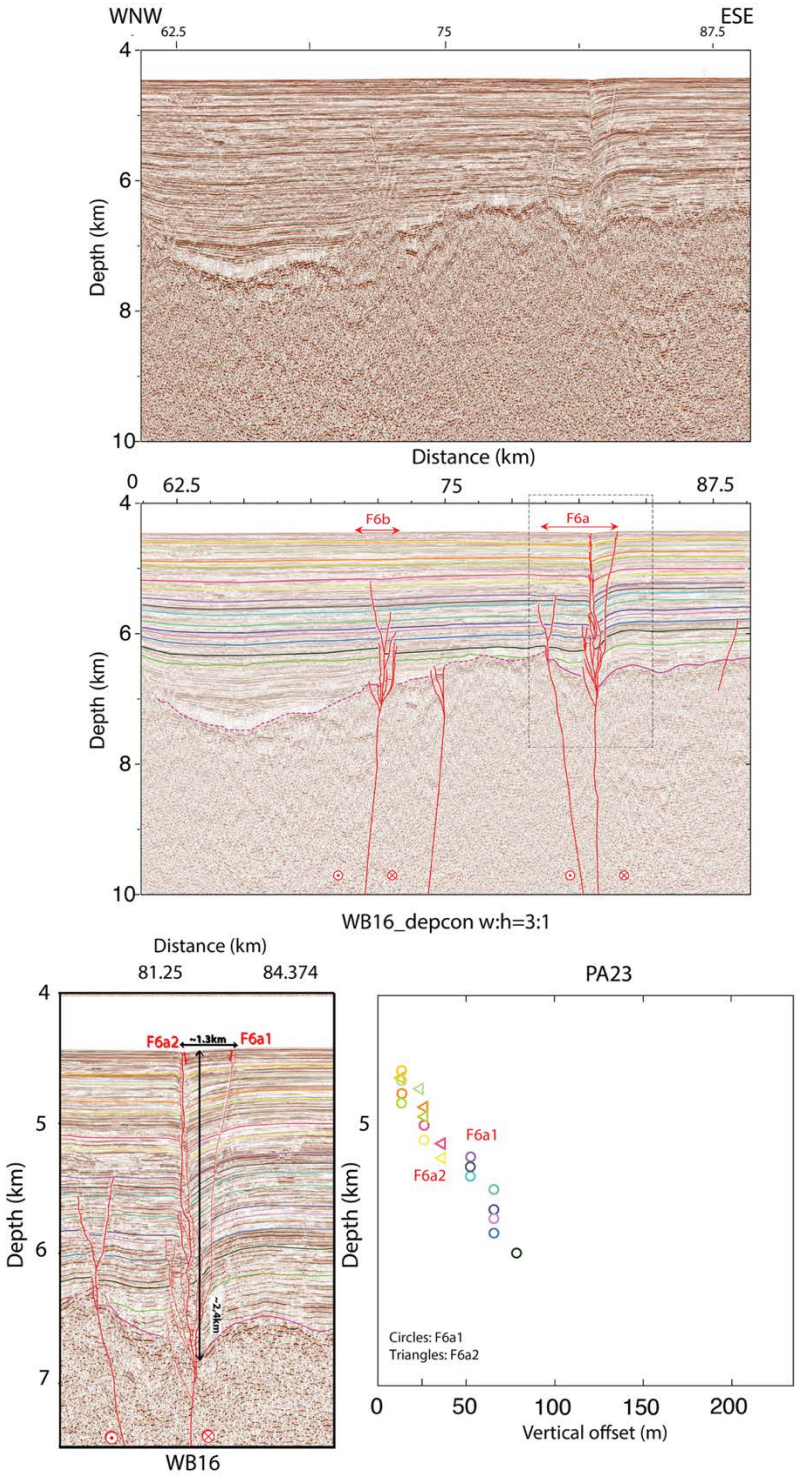

Figure S8. Seismic profile WB16 and associated cumulative vertical offset as a function of depth in the pull-apart like basin 23. *PA23 shows a clear depression/basin morphology at the surface. Two splays of the F6a FZ identified on the profile WB16 with slightly disturbed basement and sedimentary cover reflectors.*

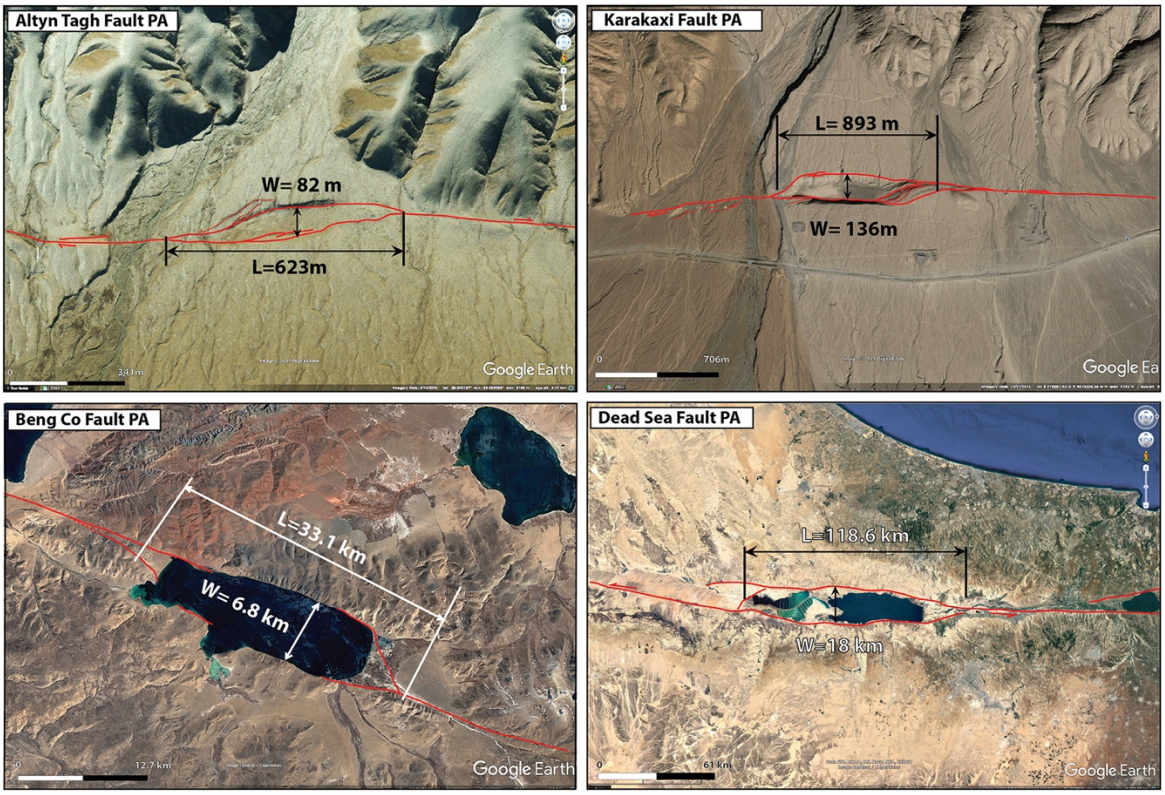

Figure S9. Geometric characteristics of continental pull-apart basins developed along main strike-slip plate measured on Google Earth imagery. *Length (L) and width (W) measurements of pull-apart basins along the Altyn Tagh fault (top left), Karakaxi fault (Top right), BengCo fault (middle segment of the Karakorum-Jiali fault system) (bottom left), and Dead Sea fault (bottom right).*

Table S1. *Pull-apart dimensions (Length, width, and depth) presented in this study.*

Table S2. *Australia/India convergence rates estimated for two locations within the composite India-Australia-Capricorn plate with plate calculator@unavco.org. AU: Australia; IN; India; EU: Eurasia; NNR: no net rotation frame. The two reference points located within AUSTRALIA and INDIA subplates for which the convergence rates are indicated here are reported in Figure 1a (as target symbols).*

Reference	Model	Plate (reference)	Latitude	Longitude	Velocity mm/yr	AU/IN Vel mm/yr	Azimuth (cw from N)	N Vel. mm/yr	AU/IN N. Vel mm/yr	E Vel. mm/yr	AU/IN E. Vel mm/yr
No net rotation frame	MORVEL 2010	AU(NNR)	*20°S*	*110°*	70.19	10.68	37.72°	55.92	18.61	42.94	-3.42
		IN(NNR)	*1.44°*	*71.83°*	59.51		51.17°	37.31		46.36	
	NUVEL 1A	AU(NNR)	*20°S*	*110°*	71.89	12.96	36.03°	58.14	17.8	42.29	-0.67
		IN(NNR)	*1.44°*	*71.83°*	58.93		46.80°	40.34		42.96	
FIXED PLATE	MORVEL 2010	AU(EU)	*20°S*	*110°*	71.73	25.88	24.59°	65.22	28.38	29.85	2.56
		IN(EU)	*1.44°*	*71.83°*	45.85		36.53°	36.84		27.29	
	NUVEL 1A	AU(EU)	*20°S*	*110°*	74.51	27.31	21.69°	69.24	27.72	27.54	5.1
		IN(EU)	*1.44°*	*71.83°*	47.2		28.39°	41.52		22.44	